

# DZHELEPOV LABORATORY OF NUCLEAR PROBLEMS

## ELEMENTARY PARTICLE PHYSICS

The main 2005 results obtained within the framework of the CDF project are the world's best top-quark mass measurements and maintaining efficient operation of the CDF. It was stated in the «FNAL Today» issues of 21 April and 28 July, 2005 that the JINR–INFN–FNAL team made a significant contribution to the world's most precise top-quark mass measurement in the so-called «lepton + jets» topology [1, 2]  $M_{\text{top}} = 173.5^{+3.7}_{-3.6}(\text{stat.}) \pm 1.3(\text{syst.})$  (Fig. 1, *a*) and improved the precision of the top-quark mass measurement in the so-called «dilepton» topology [3–5]  $M_{\text{top}} = 169.9^{+9.2}_{-9.3}(\text{stat.}) \pm 3.8(\text{syst.})$  (Fig. 1, *b*).

A new method to extract the  $M_{\text{top}}$  is proposed by the University of Athens/Dubna group. The trans-

verse momentum of electrons and muons produced in  $t\bar{t} \rightarrow$  dilepton and the  $t\bar{t} \rightarrow$  lepton + jets channels is sensitive to  $M_{\text{top}}$  and can be accurately measured [6, 7] with a very small systematic error and, at large enough integrated luminosity, with a very small total error. The method is not affected by uncertainties in the jet energy scale and in  $b$ -tagging and is applicable to both the Tevatron and the LHC collider experiments.

In 2006 the JINR/CDF group plans to considerably reduce the error of the  $M_{\text{top}}$  to a level of  $2 \text{ GeV}/c^2$ , which will enable us to establish a new limit on the Higgs mass, and to measure the top-quark charge to make sure that it is consistent with the SM.

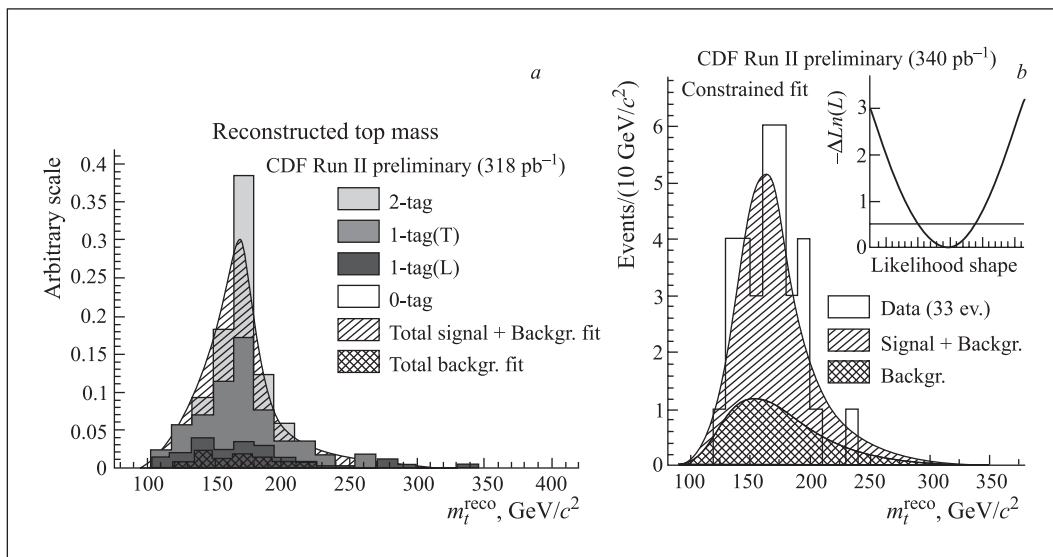


Fig. 1. Reconstructed top mass for the «lepton + jets» mode (*a*) and dilepton mode (*b*)

In the year 2005 the **D0** experiment accumulated more than  $1 \text{ fb}^{-1}$  as written on the tapes. The JINR group contributed greatly to this success by supporting the D0 forward–backward muon tracking system. Concerning the physics analysis, the group continues the search for  $\chi_b$  baryon by developing dedicated algorithms and the study of direct photon production aimed at jet energy scale calibration and determination of the gluon distribution function. The first important result obtained in this way with a leading contribution of the JINR/DLNP group is the inclusive measurement of the isolated photon cross section.

In high-energy  $p\bar{p}$  collisions the dominant source for production of photons with a moderate and high transverse momentum  $p_T^\gamma$  is direct (or prompt) photons. They are called direct since they are produced directly from parton–parton interactions and not from decays of hadrons (such as  $\pi^0, \eta, K_S^0$ ). These photons come unaltered from the hard process and therefore can allow a test of the hard scattering dynamics. Direct-photon production is complementary to deep inelastic scattering, Drell–Yan pair production, and inclusive production of jets. Identification of photons is free from uncertainties caused by fragmentation of partons into hadrons or by experimental issues related to jet identification and energy measurement, and thus has an advantage over jet production measurement. In the region up to  $p_T^\gamma \cong 150 \text{ GeV}$  direct photons are mainly produced through the Compton scattering  $qg \rightarrow q\gamma$  and thus their production cross section is sensitive to the gluon density inside the colliding hadrons. A high centre-of-mass energy at the Tevatron and the statistics accumulated currently in Run II allow one to test quantum chromodynamics (QCD) and gluon distribution in the region of large  $Q^2$  and in a wide range of  $x_T$ :  $0.02 < x_T < 0.30$ . Measurements of the isolated photon cross section also enable tests of the next-to-leading order (NLO) and resummed QCD calculations, phenomenological models of gluon radiation, studies of photon isolation and the fragmentation process. In addition, photons in the final state may be an important signpost to new particles and/or physics beyond the Standard Model. For this reason it is necessary to study and to understand the «conventional» sources of photons. Unfortunately, this measurement is complicated by the presence of energetic neutral mesons, produced in the core of hadronic jets that mimic the photon signal. But the selection criteria (including the photon isolation) and the identification method that have been found make it possible to get rid off the background events and to register the photon signal with a reasonable accuracy.

In D0 the photon production cross section has been measured over a wide range of the photon transverse momentum  $p_T^\gamma$ ,  $23 < p_T^\gamma < 300 \text{ GeV}$  (Fig. 2), which significantly (a factor of  $\sim 2.5$ ) extends previous measurements. In the presented  $p_T^\gamma$  interval the photon cross section falls by more than five orders of magnitude. The uncertainties of the measurement are comparable with

the existing theoretical ones. It has been concluded that the photon cross section found agrees with the theoretical predictions in the entire  $p_T^\gamma$  interval within uncertainties. There were just five events with  $p_T^\gamma > 300 \text{ GeV}$  (which were not used in this analysis), but due to increasing Tevatron luminosity one can expect much more statistics in the coming 2–3 years [8]. It would allow one to study the region up to  $p_T^\gamma \cong 500\text{--}600 \text{ GeV}$  and to check predictions of the «standard» theory, as well as to look for possible «traces» of new physics.

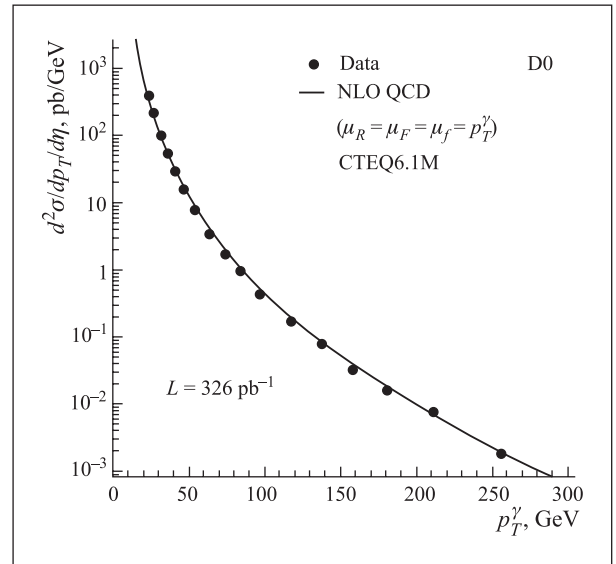


Fig. 2. Inclusive cross section for production of isolated photons as a function of  $p_T^\gamma$ . The results from the NLO pQCD calculations are shown by the solid line

All data collected in 2001–2003 within the framework of the **DIRAC** experiment were processed with the updated program and constants. The design of the setup, including dimensions of all detectors, was revised to allow for the kinematics of  $\pi^\pm K^\mp$  atoms and the particle identification system. The new vacuum channel was designed and manufactured at JINR. New readout electronics which will be used for almost all scintillation detectors is designed and prototypes are being manufactured. The precise measurement of the multiple scattering in thin scatterers was performed. Sixty percent of all drift chambers are already repaired, the rest will be repaired before the run in 2006. Production of long-lived states of  $\pi^+\pi^-$  atoms was studied [9]. A new Scintillating Fiber Detector (SFD) with fibers 0.27 mm in diameter was designed and its electronics prototype was designed and manufactured. A heavy-gas Cherenkov counter for pion identification was designed. A new trigger system was devised and part of the new DAQ was designed and constructed.

In 2006 it is planned to analyze all data collected in 2000–2003 in the lifetime measurement with a statistical accuracy of about 10% on the Ni and Ti targets

to evaluate systematic errors in the lifetime, to manufacture detectors and electronics to upgrade the setup, and to install and tune all new and modified detectors, the readout system, the trigger and the DAQ. The first run with the modified setup for calibration and data taking for observation of the  $\pi^+\pi^-$  atom in the long-lived states is under preparation.

New data on the cross section of the positive pion production were obtained with the **HARP** forward spectrometer for K2K beam line [13]. The neutrino beam of the K2K experiment originates from the decay of light hadrons produced by exposing an aluminium target to a proton beam of momentum 12.9 GeV/c. The tracking of forward-going particles in the forward spectrometer is performed by a set of large ( $3 \times 3$  m) drift chambers (NDCs). Twenty-three NDCs were placed upstream and downstream of the 0.5 T dipole magnet. The  $\pi^+$ -production data were fitted with the Sanford–Wang parametrization. The HARP cross-section mea-

surement is shown in Fig. 3 (data points with error bars), in comparison with the best Sanford–Wang parametrization fit (histograms). A detailed error analysis was performed. The total uncertainty for the pion production cross section measured over the entire phase space ( $0.75 < p < 6.5$  GeV/c) and ( $30 < \theta < 210$  mrad) is estimated to be 5%.

The HARP cross-section measurements were used to make a new prediction for the ratio of neutrino fluxes at the «far» and «near» detectors of the K2K experiment (Fig. 4). This quantity is defined as the ratio of fluxes in the absence of neutrino oscillation effects. Figure 5 shows the energy dependence of the predicted ratio based on the HARP data in comparison with the prediction used up to now by the K2K collaboration. The points with error bars are based on the HARP data. In the future, more precise HARP measurements of the far/near ratio will be used to reduce the error of neutrino oscillation parameters in the K2K experiment.

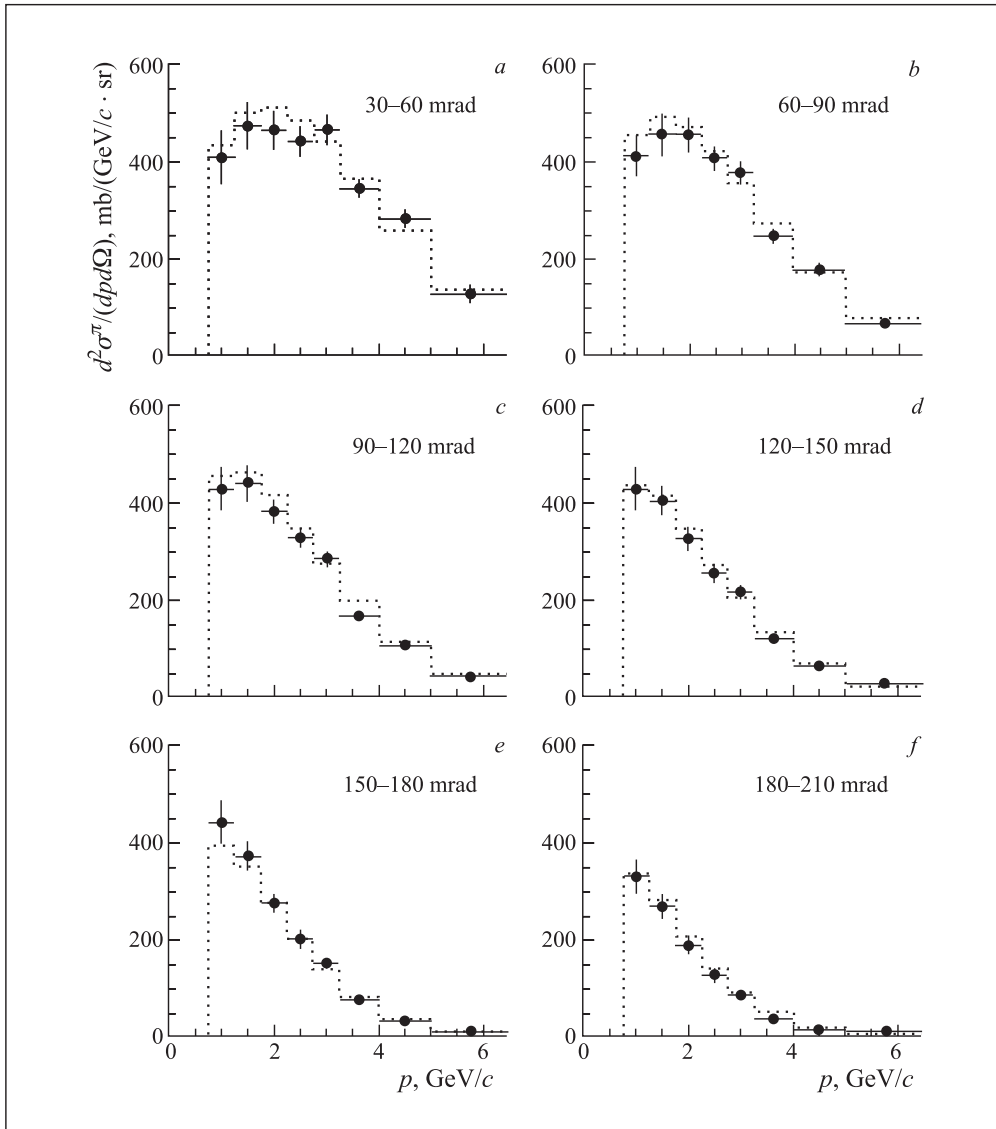


Fig. 3. Measurement of the double differential  $\pi^+$ -production cross section  $d^2\sigma^{\pi^+}/dpd\Omega$  for incoming protons of 12.9 GeV/c on an aluminium target as a function of the pion momentum, in bins of pion polar angle  $\theta$

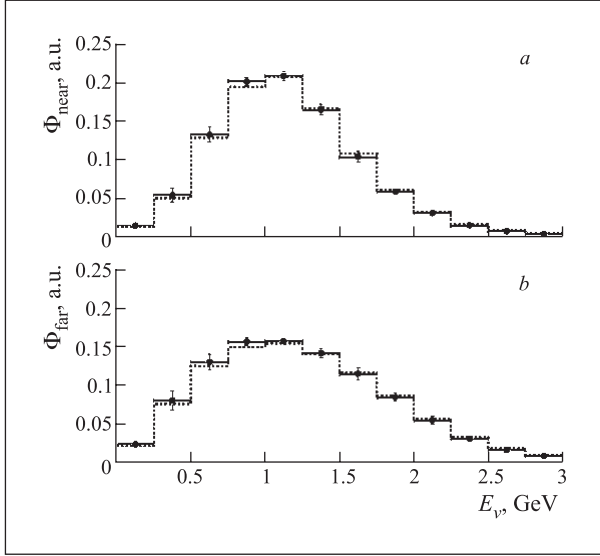


Fig. 4. Unit-area normalized flux predictions at the K2K near (a) and far (b) detector locations, respectively. Dotted histograms are for the hadron model predictions, filled circles are for measurements

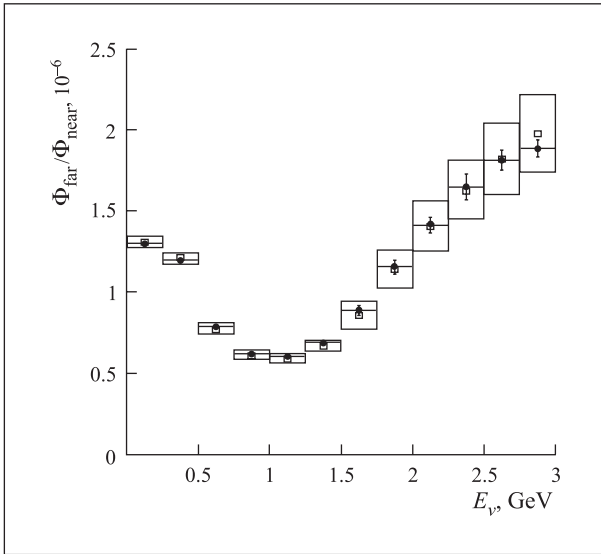


Fig. 5. Muon neutrino fluxes in the K2K experiment as a function of the neutrino energy, as predicted by the default hadronic model assumptions in the K2K beam Monte Carlo simulation (dotted histograms) and by the HARP  $\pi^+$ -production measurement (filled circles with error bars)

In 2006 the collaboration plans to measure the cross section of hadron production at the proton momentum 8.9 GeV/c on the Be target for the analysis of the Mini-Boone experiment at Fermilab (USA), to measure the forward and large-angle  $\pi^\pm$  spectra in collisions of proton of energy up to 8 GeV/c with the Ta target for designing the proton driver of a Neutrino Factory Project, to measure the spectrum of  $\pi^\pm$  in interaction of protons of momentum 1.5 GeV/c with water targets, to try to

explain the anomalous  $\bar{\nu}_e$  signal reported by the LSND collaboration.

For the **ATLAS Hadron Tile Calorimeter**, particular attention was given to the R&D and the quality control methods; it was recognized that the JINR-created laser metrology plays an important role in ensuring high-precision assembly of the calorimeter submodules and modules.

To establish the electromagnetic scale and to understand the response of the ATLAS Tile hadronic Calorimeter to electrons, 12% of the modules were exposed to electron beams with various energies in three possible ways: cell scan at  $\Theta = 20^\circ$  at the centres of the front face cells,  $\eta$ -scan and tilerow scan at  $\Theta = 90^\circ$  for the module side cells. The work of the JINR group is devoted to the determination of the electromagnetic energy calibration constants of the EBM- (ANL-44), EBM+ (IFA-42), BM (JINR-55) TILECAL modules at energies  $E = 10, 20, 50, 100$  and 180 GeV and  $\Theta = 20^\circ$  and  $\Theta = 90^\circ$  and  $\eta$ -scans on the basis of the July 2002 testbeam run data using the flat filter [10] and fit filter [11] methods of the PMT signal reconstruction. The average electron calibration constants obtained by the flat filter method are equal to  $1.157 \pm 0.002$ ,  $\text{RMS} = (2.6 \pm 0.2)\%$  for  $\Theta = 20^\circ$ ,  $1.196 \pm 0.005$ ,  $\text{RMS} = (5.7 \pm 0.3)\%$  for  $\Theta = 90^\circ$  and  $1.143 \pm 0.005$ ,  $\text{RMS} = (3.7 \pm 0.3)\%$  for  $\eta$ -scan. The average electron calibration constants obtained by the fit filter method are  $1.046 \pm 0.002$ ,  $\text{RMS} = (3.0 \pm 0.2)\%$  for  $\Theta = 20^\circ$ ,  $1.082 \pm 0.004$ ,  $\text{RMS} = (5.3 \pm 0.3)\%$  for  $\Theta = 90^\circ$ ,  $1.046 \pm 0.004$ ,  $\text{RMS} = (3.8 \pm 0.3)\%$  for  $\eta$ -scan. In [12] the electron energy resolutions of the EBM- (ANL-44), EBM+ (IFA-42) and BM (JINR-55) modules of the ATLAS Tile Calorimeter at the energies 10, 20, 50, 100 and 180 GeV and  $\Theta = 20^\circ$  and  $\Theta = 90^\circ$  and  $\eta$ -scan were extracted from the July 2002 testbeam run data using the flat filter method of the PMT signal reconstruction. The parameters of the electron energy resolution for the quadratic fit are  $a = (29 \pm 1.6)\% \sqrt{\text{GeV}}$ ,  $b = (3.0 \pm 0.4)\%$  at  $\Theta = 20^\circ$  and  $a = (22 \pm 1)\% \sqrt{\text{GeV}}$ ,  $b = (2.3 \pm 0.3)\%$  at  $\Theta = 90^\circ$ . The energy resolution results were compared with the Monte-Carlo-based parametrization. Good agreement is observed for the linear fit. The calibration constants obtained are included in the TILECAL calibration database, ATLAS software and will be used for the energy calibration of the ATLAS Tile hadronic calorimeter.

Within the **SANC** project, the team members worked in 2005 on creation of new FORM programs for calculation of  $F \rightarrow 3f$  decays and  $f\bar{f} \rightarrow b\bar{b}$  processes at the one-loop level; on CC and NC Drell-Yan processes at LHC; on interfacing libraries of partonic densities to the SANC environment; on implementation of soft and hard bremsstrahlung contributions for various  $2 \rightarrow 2$  processes.

SANC version v1.00 is available from servers at Dubna <http://sanc.jinr.ru/> (159.93.75.10) and CERN

<http://pcphysanc.cern.ch/> (137.138.180.42). The system is being more and more widely used for physical applications. The one-loop electroweak corrections to the charged current Drell–Yan processes were revised within the automatic SANC system [14]. Contributions with mass singularities were treated with allowance made for higher-order leading logarithmic corrections. The theoretical accuracy in the description of the processes was studied. In [15] the implementation of the processes  $f_1\bar{f}_1ZZ \rightarrow 0$  and  $f_1\bar{f}_1HZ \rightarrow 0$  within the framework of SANC system was described ( $f_1$  stands for a massless fermion whose mass is kept nonzero only in arguments of log functions and  $\rightarrow 0$  means that all 4-momenta flow inwards).

During the year 2006 the SANC system is supposed to be extended to more complicated processes. In particular, it is planned to complete calculations of the  $H \rightarrow 4\mu$  process in the one- $Z$  resonance approximation and to implement several QCD processes. It is also planned to calculate the decay  $H \rightarrow 2\mu 2\nu$  in the one- and double- $W$  resonance approximation, to calculate the process  $f\bar{f} \rightarrow HW$  at the one-loop level, to calculate the processes  $gg \rightarrow BB$ ,  $\gamma\gamma \rightarrow BB$  ( $BB = Z, \gamma, H, W$ ) at one-loop level, to create environment for one-loop calculations of the  $5 \rightarrow 0$  processes and apply it for the complete calculations of the decay  $H \rightarrow 4f$ .

The TUS space experiment was proposed to address some of the most important astrophysical and particle physics problems. It is aimed at measuring the energy spectrum, composition, and angular distribution of the Ultra High Energy Cosmic Rays (UHECR) at  $E \approx 10^{19}–10^{20}$  eV to study the region of GZK cut-off. The R&D stage of the TUS project is close to the end. At present the first prototypes of the detector are under testing and the space mirror-concentrator is being developed. The launch of the MSU satellite Tatiana was used to test the TUS photosensors and their electronics and to measure the UV light emitted by the Earth atmosphere. The Tatiana satellite was launched on 20 January 2005. The energy resolution of fluorescence detectors is heavily related to the uncertainties in

the fluorescence production yield. Now the collaboration of the JINR (Dubna) and LAPP (Annecy, France) scientific groups is performing measurement of the fluorescent light yield [16–18].

In 2006 the collaboration plans to complete R&D on the Fresnel mirror for the TUS ground prototype, to finish the design and production of a special tool for Fresnel mirror measurements.

The aim of the NUCLEON project is direct CR measurements in the energy range  $10^{11}–10^{15}$  eV and charge range up to  $Z \approx 40$  in the near-Earth space to resolve mainly the knee problem in the CR spectrum. JINR is particularly interested in the search for a signal of production of heavy particles with  $M \approx 0.5$  TeV as expected for the lightest and stable SUSY or WIMP particle that is needed for the dark matter understanding. The first full-scale double-sided trigger module of the NUCLEON trigger system was designed and produced. The second prototype is under development now.

In 2006 it is planned to design, produce and test the trigger system prototype of the NUCLEON detector, to develop the MC-simulation program for the NUCLEON trigger system, and to design, produce and test the prototype FE electronics of the trigger system.

The HYPERON experiment is aimed at studying nuclear transparency dependence on the atomic number and colour screening effects in charge-exchange reactions with neutral mesons in the final state. A new data acquisition system was developed which allows collecting experimental data at a very high speed of 9 Mbyte/s. It means that one can record practically all events which pass the trigger. The data acquisition system was tested on the calorimeter in the HYPERON-M experiment in the December 2004 run.

In December 2004, data taking was started but without using proportional chambers and tagging system. About  $1.8 \cdot 10^7$  trigger events with Be, Al and Cu targets were collected. Preliminary data processing was done, which showed that harder trigger conditions should be set to reject the background. The data from three targets are not enough to get reliable information about  $A$ -dependence of the nuclear transparency.

## LOW- AND INTERMEDIATE-ENERGY PHYSICS

The NEMO-3 detector located at the Modane underground laboratory (LSM, France, 4800 m w.e.) is searching for neutrinoless double beta decay ( $0\nu 2\beta$ ), which would be an indication of new fundamental physics beyond the Standard Model, such as the absolute neutrino mass scale, the nature of neutrino (either Dirac or Majorana), and neutrino hierarchy. The main goal of the NEMO project is to reach the 0.1–0.3 eV sensitivity for the effective Majorana neutrino mass  $\langle m_\nu \rangle$  ( $T_{1/2}^{0\nu 2\beta} (100\text{Mo}) \sim 10^{25}$  y).

During 2005, data collection from the NEMO-3 detector was continued in a regular mode under stable conditions. New statistics ( $\sim 236$  effective days of data taking since the beginning of 2005) is free from the radon background, which was highly suppressed by the end of the first stage of the experiment. The total NEMO-3 exposure is 762 days since February 2003. Data analysis of Phase I of the experiment (2003–2004) was performed during 2005 [19]. After analysis of the data collected for 389 days no evidence of  $0\nu 2\beta$  was

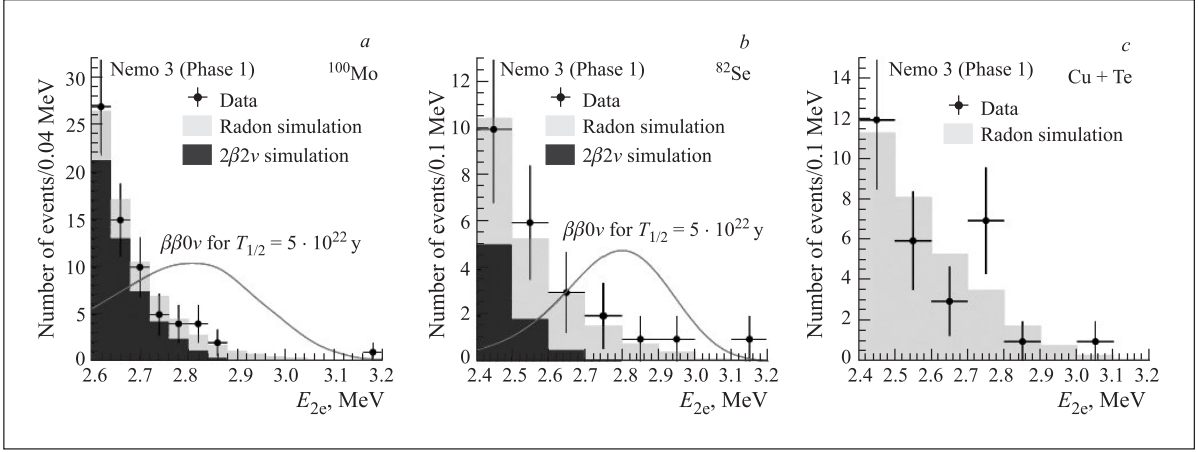


Fig. 6. Spectra of the energy sum of two electrons in the  $0\nu\beta\beta$ -energy window after 389 effective days of data collection from February 2003 till September 2004 (Phase I): *a*) with 6.914 kg of  $^{100}\text{Mo}$ ; *b*) with 0.932 kg of  $^{82}\text{Se}$ ; *c*) with copper and tellurium foils. Shaded histograms are Monte-Carlo simulated backgrounds: dark is the  $2\nu\beta\beta$  contribution and light is the radon contribution. The solid line corresponds to the expected  $0\nu\beta\beta$  signal if  $T_{1/2}^{0\nu\beta\beta} = 5 \cdot 10^{22}$  y

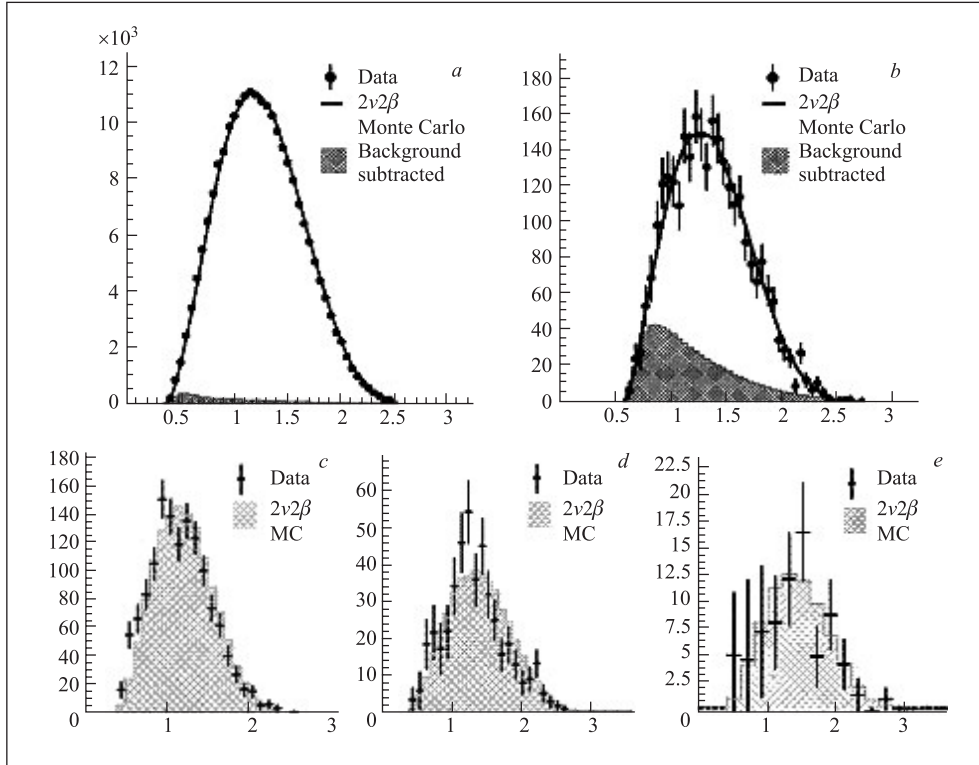


Fig. 7. Energy sum spectra of two electrons emitted in  $2\nu\beta\beta$  decay of some isotopes. Points are experimental data, the expected simulated  $2\nu\beta\beta$  signal is shown by a histogram, the subtracted background is shown by a shaded histogram. Energy in MeV is pointed on the  $x$  axis, the number of events is plotted on the  $y$  axis. *a*)  $^{100}\text{Mo}$ , exposure 7.37 kg · y, 219000 events, signal-to-background ratio (S/B) is 40. *b*)  $^{82}\text{Se}$ , exposure 1.0 kg · y, 2750 events, S/B is 4. *c*)  $^{116}\text{Cd}$ , exposure 0.2 kg · y, 1371 events, S/B is 7.5. *d*)  $^{150}\text{Nd}$ , exposure 17 g · y, 449 events, S/B is 2.8. *e*)  $^{96}\text{Zr}$ , exposure 4.3 g · y, 72 events, S/B is 0.9

found either in  $^{100}\text{Mo}$  or in  $^{82}\text{Se}$  (Fig. 6) within the limits (90% C.L.):

$$T_{1/2}^{0\nu\beta\beta} (^{100}\text{Mo}) \geq 4.6 \cdot 10^{23} \text{ y} \Rightarrow \langle m_\nu \rangle \leq 0.7\text{--}2.8 \text{ eV},$$

$$T_{1/2}^{0\nu\beta\beta} (^{82}\text{Se}) \geq 1.0 \cdot 10^{23} \text{ y} \Rightarrow \langle m_\nu \rangle \leq 1.7\text{--}4.9 \text{ eV}.$$

NEMO-3 is also sensitive to other possible  $0\nu\beta\beta$  mechanisms. On the assumption of gluino or neutralino ex-

change, a limit on the trilinear  $R$ -parity-violating supersymmetric coupling  $\lambda_{111} < 1.6 \cdot 10^{-4}$  for  $^{100}\text{Mo}$  is obtained. On the assumption of a right-handed weak current, the limit is  $T_{1/2}^{0\nu\beta\beta} (^{100}\text{Mo}) = 1.7 \cdot 10^{23}$  y at 90% C.L. corresponding to an upper limit on the coupling constant of  $\lambda < 2.5 \cdot 10^{-6}$ . The analysis of  $2\nu\beta\beta$  decay of a set of isotopes was also done (Fig. 7). A real estimate of the final NEMO-3 sensitivity was obtained

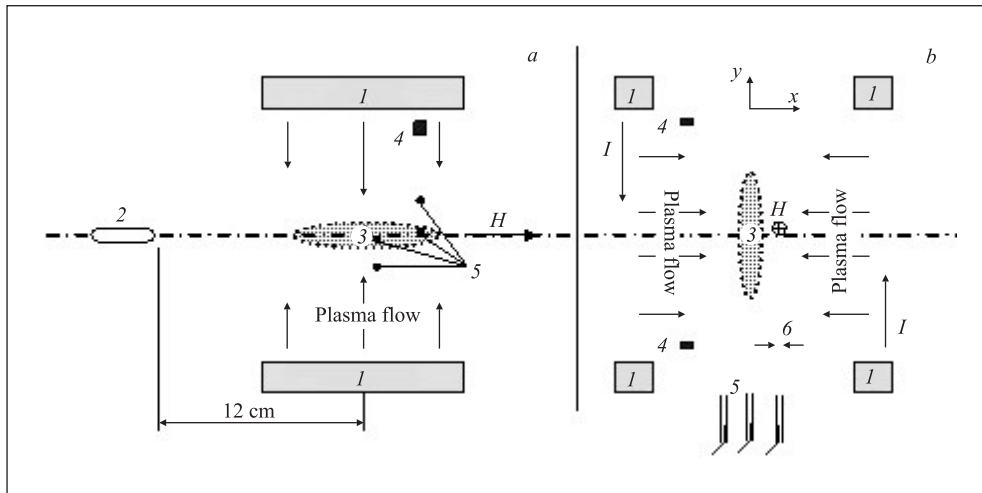


Fig. 8. Schematic of the experimental setup in two projections: *a)* view along the  $B$  field; *b)* side view normal to the  $B$  field:  $I$  — HV discharge electrodes; 2 — spectrometer; 3 — collision region of plasma flows; 4 — voltage plate electrodes; 5 — light detector collimators; 6 — floating probes

with allowance made for the directly measured background. After five years of data collection (in 2009) the expected sensitivity at 90% C.L. will be  $T_{1/2}^{0\nu 2\beta}({}^{100}\text{Mo}) \geq 2.0 \cdot 10^{24}$  y, leading to  $\langle m_\nu \rangle \leq 0.3\text{--}1.3$  eV, which complies with the project goal and is at the level with the world's best results obtained up to now. R&D of the next-generation SuperNEMO  $0\nu\beta\beta$  project is under way in parallel with NEMO-3 data processing.

In 2006 the collaboration is going to continue NEMO-3 data taking with emphasis placed on improvement of the  $0\nu\beta\beta$  sensitivity, and data analysis, and to publish results for  $2\nu\beta\beta$  transitions to excited states of  ${}^{100}\text{Mo}$ ,  $2\nu 2\beta$  decay of  ${}^{48}\text{Ca}$  and other isotopes. A three-year SuperNEMO R&D program will be launched. The JINR group will focus on R&D of the calorimeter making and testing new plastic scintillators. One of the most important R&D goals is improvement of the energy resolution of the calorimeter up to 7% at 1 MeV (against 15–17% in NEMO-3). Other tasks are R&D for radon monitoring, software development, and simulations in order to optimize the design of the SuperNEMO module.

Investigation of reactions between light nuclei at the keV energy level is of great importance because it could provide direct verification of fundamental symmetries in strong interactions, such as charge symmetry, isotopic invariance, input of the meson currents, effect of screening of nuclei, etc. It could also help to solve a number of astrophysical problems. At present the LESI collaboration carries out the research on the generation of colliding plasma fluxes in the keV energy range and continues the nuclear reaction investigations at the astrophysical range energies at the Research Institute of Nuclear Physics at the Polytechnic University (Tomsk) (Fig. 8). It is shown that the efficiency of converting

the energy introduced in the discharges into the directed motion of plasma is 0.3–0.6 and the total number of particles in the fluxes is  $10^{19}$  per pulse.

In addition, the collaboration is developing a new type of plasma accelerator based on the Hall ion source. It is anticipated that the Hall accelerator will be able to generate intense plasma flows ( $I = 10$  A/cm<sup>2</sup>) with small ion energy spread. This will allow more precise information about characteristics of nuclear reactions at ultralow energies. A distinctive feature of the proposed methods is that they hold promise for the study of strong interactions between light nuclei at ultralow energies, because there is a real possibility of substantially decreasing the lower measurement range for the astrophysical  $S$  factor and nuclear reaction cross sections  $\sigma \sim 10^{-33}\text{--}10^{-37}$  cm<sup>2</sup> [20, 21].

In 2006 the collaboration will continue the creation of the Hall plasma accelerator and the precision study of the dependence of astrophysical  $S$  factors and cross sections for the  $pd$  reaction on the collision energy in the range of 2–12 keV. It is also planned to measure characteristics of the nuclear  $dd$  reaction in the astrophysical deuteron collision energy range by using plasma counter fluxes.

In 2005 experimental pion radiative decay (PRD) data, obtained by the PIBETA collaboration in 2004 in a special experiment, were analyzed. Necessity of the new experiment was caused by the fact that in the 1999–2001 experiment the number of PRD events registered in a certain kinematic region «B» (defined by the relative angle between the gamma quantum and the positron  $\theta_{\gamma,e} > 40^\circ$ , gamma-quantum energy  $E_\gamma > 55.6$  MeV, and positron energy  $E_e > 20$  MeV), was  $\sim 20\%$  smaller than the Standard Model predicted.

The new data were obtained on the PSI pion beam with a stopping rate of 50–100 KHz. Such an inten-

sity allowed the accidental coincidence background rate to be reduced by a factor  $\sim 10$  in comparison with the measurements of 1999–2001 devoted to examination of the pion beta decay (the RPD data were only a by-product). To obtain more reliable results, the collaboration decided to analyze the new data independently by two groups of physicists (from Virginia and from Dubna). The Dubna physicists have no previous experience of such an analysis. It is necessary to note that the

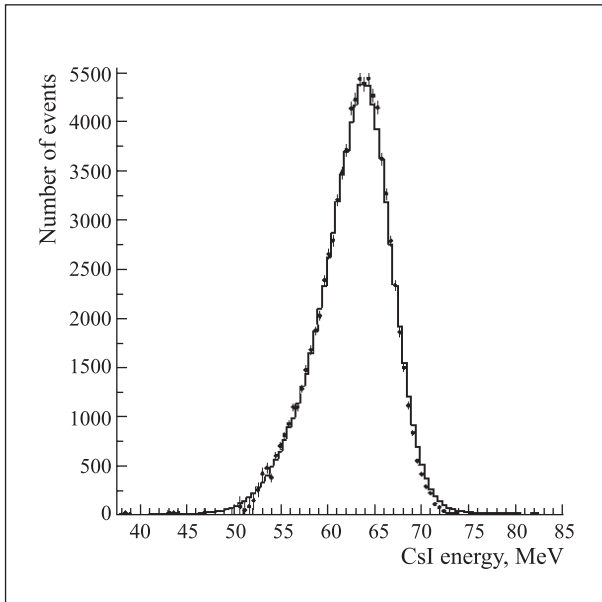


Fig. 9. Spectrum of positrons from the  $\pi^+ \rightarrow e^+\nu$  decay. The continuous curve is the Monte Carlo simulation

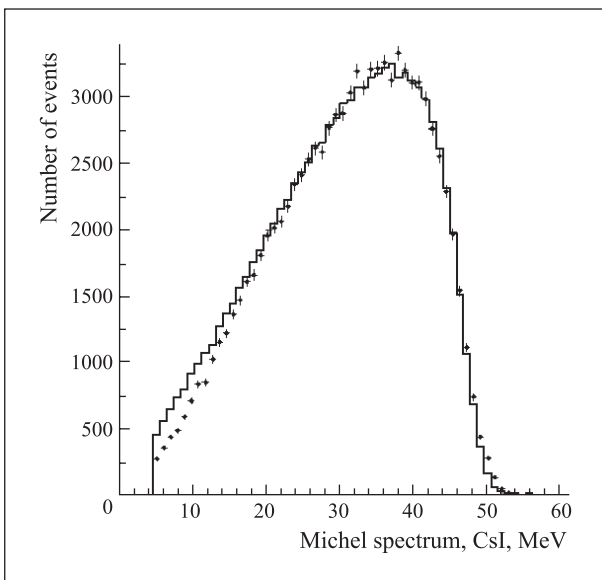


Fig. 10. Spectrum of positrons from the  $\mu^+ \rightarrow e^+\nu\bar{\nu}$  decay. The continuous curve is the Monte Carlo simulation

analysis of the data is a very delicate and difficult task demanding extremely precise account of many various factors. During the year under review a preliminary

analysis of the entire experimental PRD data set (corresponding to  $\sim 6.12 \cdot 10^{11}$  pion stops) was made. The  $\pi^+ \rightarrow e^+\nu$  and  $\mu^+ \rightarrow e^+\nu\bar{\nu}$  decays were studied. These processes are used to calibrate the data on the  $\pi^+ \rightarrow e^+\nu\gamma$  decay [22]. About 240000  $\pi^+ \rightarrow e^+\nu$  decays were analyzed. The positron energy spectrum for this decay is shown in Fig. 9. In Fig. 10 the measured spectrum of positrons from the  $\mu^+ \rightarrow e^+\nu\bar{\nu}$  decay is shown. It is evident from the figures that the measured spectra are in good agreement with the simulated ones. There were found 17085 RPD events. Of them 7261 events fall within kinematic region B where the deficit of events was earlier observed. For the gamma quanta registered with energy exceeding  $\sim 60$  MeV, the  $\sim 11\%$  deficit of events is observed at a statistical measurement accuracy of  $\sim 2\%$ . It is important to underline that the data analysis is not yet fully completed, all current results are preliminary and any conclusion concerning existence of the anomaly would be premature. The number of events identified as the  $\pi^+ \rightarrow e^+\nu$  decay depends on the adequacy of the computer simulation of real processes, the precision of the calibration parameters and the background suppression efficiency. The systematic errors determining the overall precision of the experiment depend on perfection of these procedures.

In 2006 the detailed analysis of the 2004 experimental data on radiative decay of the pion will be continued. A publication concerning the results of the experiment will be prepared. It is planned to upgrade the PIBETA detector and to optimize the pion beam for more precise experimental investigation of the  $\pi^+ \rightarrow e^+\nu$  and  $\pi^+ \rightarrow e^+\nu\gamma$  decays.

Within the framework of the **CATALYSIS** project a paper [23] on analysis of D–T muon catalyzed fusion (MCF) data was prepared. First preliminary results were obtained in T–T catalysis data handling, data

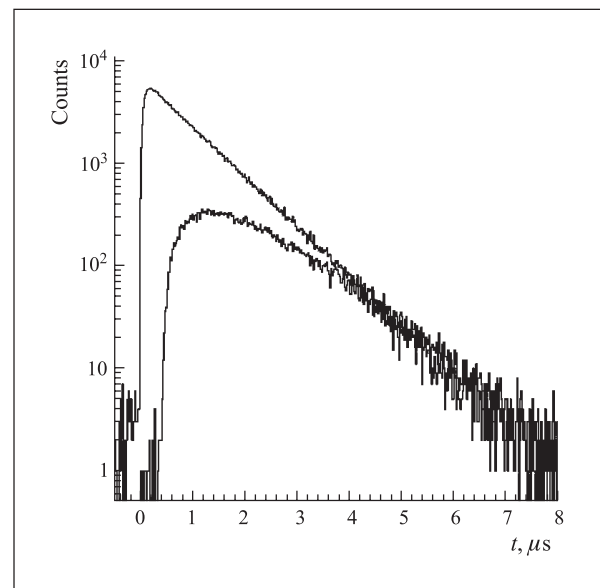


Fig. 11. Time distributions of the first and second registered neutrons from T–T catalysis

processing by an independent method is in progress. The experimental time distributions of the first and second registered neutrons (from catalysis) are shown in Fig. 11. The experiment on radiative deuteron capture from the state of the mesomolecule  $dd\mu$  is under preparation: a unique detector of  $\gamma$  quanta is installed, which includes a BGO crystal 130 mm in diameter and 60 mm high, immersed (for background suppression) in the plastic scintillator; a high-pressure deuterium target is designed.

In 2006 the collaboration plans to finish T–T catalysis data handling in order to obtain the parameters of muon catalyzed fusion in tritium and the information about the mechanism of the reaction with possible  $n$ – $n$  and  $n$ – $\alpha$  correlations and to perform a complex study of the parameters of the gamma detector (analysis programs, calibration and line shape, effectiveness of external background discrimination).

At the ANKE spectrometer (COSY, FZ-Jülich) the angular dependence of the vector analyzing power has been measured in the reaction  $p \uparrow + d \rightarrow (pp)_S$  at 0.5 and 0.8 GeV [24]. Proton pairs  $(pp)_S$  were selected with low kinetic energy of relative movement, lower than 3 MeV, which determined the  $^1S_0$  state of the pairs. Kinematical conditions for this quasi-binary reaction were chosen similar to those for the backward elastic  $pd$  scattering. It provides rather high momentum transfers in the process at energies in the range 0.5–2.0 GeV and a possibility of studying short-range interactions in the three-nucleon system. Registration of the isotriplet state of the final nucleon pair instead of the isosinglet in the elastic  $pd$  scattering significantly simplifies dynamics of the process [25]. It makes the process preferable as a tool for the study of a validity limit for the traditional meson–nucleon approach and for the search for a manifestation of QCD degrees of freedom in the few-nucleon interactions. A meson–nucleon model (ONE +  $\Delta$  +  $SS$ ) was found capable of describing the energy dependence of the spin-averaged differential cross section in the energy range 0.6–1.9 GeV [26], but it fails to reproduce the polarization data obtained. More refined information on the spin structure of the  $\Delta$ -excitation mechanism is required for the data description. In this respect, more conclusive data may be obtained in measurement of the deuteron tensor analyzing power planned at ANKE in 2006. Such experiments will be performed with the use of a polarized-deuteron atomic beam source target installed at ANKE in 2005.

Search for double electron capture of  $^{106}\text{Cd}$  was performed at the Modane underground laboratory (4800 m w.e.), France, using a high-efficiency low-background spectrometer TGV-2 (Telescope Germanium Vertical). The spectrometer was based on 32 planar HPGe detectors with a sensitive volume of  $2040 \text{ mm}^2 \times 6 \text{ mm}$  each (about 3 kg of Ge). Foils of Cd  $\sim 50 \mu\text{m}$  thick were inserted between the entrance windows of neighboring detectors. The main exposure

of the TGV-2 experiment was started in February 2005 and used 10 g of  $^{106}\text{Cd}$  with enrichment of 75%. The search for double electron capture in  $^{106}\text{Cd}$  decay is in progress now. Some additional events above the background were obtained in the region of  $\sim 21 \text{ keV}$  (KX Pd) of the double coincidence spectrum of  $^{106}\text{Cd}$  accumulated for 6200 h (Fig. 12). They may point to the presence of the process of double electron capture of  $^{106}\text{Cd}$ . Larger statistics and highly accurate long-term background measurements are needed for the careful analysis of these events. The additional background in the region of  $\sim 23 \text{ keV}$  caused by KX rays of Cd decreases the sensitivity of the measurement. The new limit on the half-life of the  $2\nu\text{EC}/\text{EC}$  decay mode of  $^{106}\text{Cd}$   $T_{1/2} > 6.6 \cdot 10^{19} \text{ y}$  (90% C.L.) was obtained in a preliminary calculation of the experimental data. The present value is more than one order of magnitude higher than those obtained in previous experiments. The new value is close to the theoretical prediction for double electron capture of  $^{106}\text{Cd}$ . The new limits on the other branches of  $^{106}\text{Cd}$  decay —  $2\nu\beta^+/\text{EC}$  decay to the ground state of  $^{106}\text{Pd}$ ,  $2\nu\text{EC}/\text{EC}$  and  $2\nu\beta^+/\text{EC}$  transitions to the first  $2^+$ , 512 keV excited state of  $^{106}\text{Pd}$  — were also obtained [27].

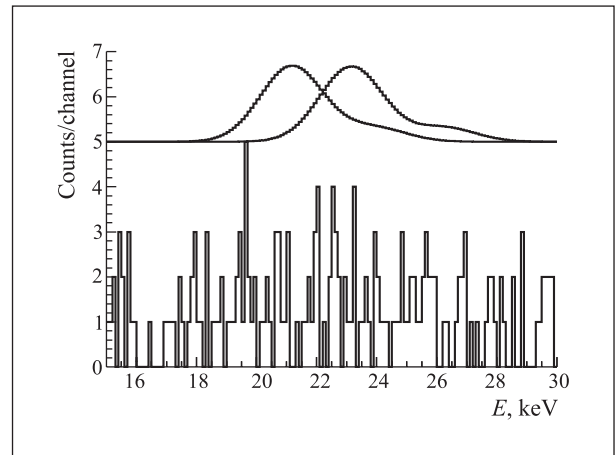


Fig. 12. Double coincidence spectrum of  $^{106}\text{Cd}$  accumulated for 6200 h

At the beginning of 2006 the measurements of  $^{106}\text{Cd}$  will be finished and the background measurement will be performed with similar samples of natural Cd. Then the study of double beta decay of  $^{48}\text{Ca}$  will be started at TGV-2.

DUBTO is a joint JINR–INFN project aimed at studying pion–nucleus interactions at energies below the  $\Delta$  resonance. The experimental device STREAMER used is a self-shunted streamer chamber filled with helium at atmospheric pressure, placed in a magnetic field, and exposed to the  $\sim 100 \text{ MeV}$  pion beam of intensity  $(1 \div 5) \cdot 10^4 \text{ s}^{-1}$  of the JINR Phasotron. The total number of  $\pi^{\pm 4}\text{He}$  events recorded during the DUBTO runs amounts to about 25000, of which about 3000 events have been processed. The main results obtained in 2005 [28, 29] include the first observation of pion

bremsstrahlung; determination of the cross sections of pion–helium reaction channels, measurement of the invariant mass  $M_{pp\pi^\pm}$  distribution in  $\pi^\pm{}^4\text{He}$  breakup reactions, measurement of the invariant  $M_{pp\pi^-}$  distribution in positive pion DCX reactions on heavy nuclei ( $^{107}\text{Ag}$ ,  $^{109}\text{Ag}$ ) in nuclear photoemulsion, pointing to existence of the so-called  $d'$  resonance (Fig. 13); estimation of the upper limit for the muon neutrino mass ( $m_\nu < 2.2$  MeV) at a 90% confidence level; this value is the lowest estimate obtained with a visualizing detector using the directly measured kinematic and dynamic parameters of the  $\pi \rightarrow \mu\nu_\mu$  decay.

In 2006 the collaboration plans to restore the spectrometer STREAMER and other DUBTO equipment damaged by the fire in April 2005, to carry out one run with a pion beam, to continue measurement and analysis of the experimental data obtained, to improve the results on the  $d'$  resonance, pion bremsstrahlung, pion absorption.

## RELATIVISTIC NUCLEAR PHYSICS

It is shown by the FASA collaboration [30, 31] that thermal multifragmentation of hot nuclei is characterized by the *two* volume (or density) parameters. It was done by analysis of the experimental data obtained with the  $4\pi$ -setup FASA for  $p(8.1 \text{ GeV}) + \text{Au}$  collisions (on the Nuclotron beam). The Statistical Multifragmentation Model (SMM) was used in this analysis. Note that only *one* size parameter is used traditionally. The existence of two different size characteristics has a transparent meaning. The first volume,  $V_t = (2.6 \pm 0.3)V_0$ , was determined from the shape of the intermediate-mass-fragment (IMF) charge distribution. This volume corresponds to the fragment formation stage, when the properly extended hot target spectator transforms into a configuration consisting of specified prefragments. They are not yet fully separated; there are links between them. The final channel of disintegration is completed during the evolution of the system up to the moment the receding and interacting prefragments become free. This is like ordinary fission. The saddle point resembles the final channel of fission by having a fairly well defined mass asymmetry. Nuclear interaction between fission prefragments ceases after descent of the system from the top of the barrier to the scission point. The size parameter obtained from the IMF charge distribution can hardly be called a freeze-out volume. It is proper to use the term «transition state volume» as in the case of ordinary fission.

Another way to find the size of the system is analysis of the fragment kinetic energy spectra. As a result, the mean volume of the system is found to be five times larger than the normal one:  $V_t = (5 \pm 1)V_0$ . The larger value of the size parameter obtained is a consequence of the main contribution of Coulomb repulsion to the IMF

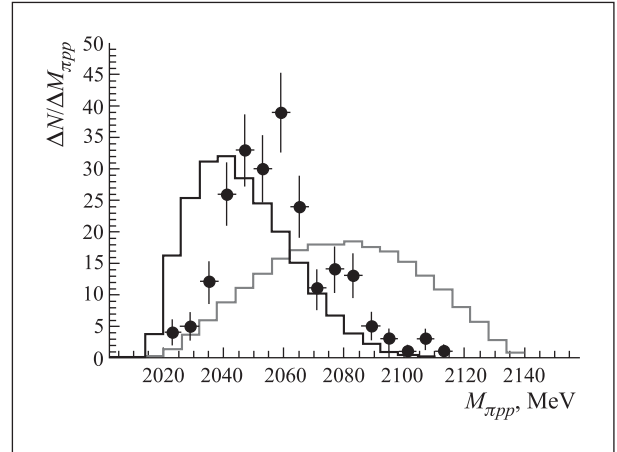


Fig. 13.  $pp\pi^-$  invariant mass distribution. The measured spectrum is shown by dots with error bars

energy, which starts to work when the system passed the «multiscission point». Thus, it is the freeze-out volume for multifragmentation in  $p + \text{Au}$  collisions. It means that the nuclear interaction between fragments is still significant when the system volume is equal to  $V_t$ , and only when the system has expanded to  $V_f$ , the fragments are frozen out.

Figure 14 illustrates the evolution of the system during the multifragmentation process. The evidence for the existence of two characteristic volumes of multifragmentation changes the understanding of the time scale of the process (see Fig. 14, *b*). Now one can imagine the following ingredients of the time scale:  $t_1$  — the mean thermalization time of the excited target spectator,  $t_2$  — the mean time of the expansion to reach the transition state,  $(t_3 - t_2)$  — the mean time of descent of the system from the top of the barrier to the multiscission point. The system configuration on the way to the scission point is composed from several prefragments connected by necks. Their random rupture is characterized by the mean time  $\tau_n$ , which is an important ingredient of fragment emission time  $\tau_{\text{em}}$ . Another ingredient of  $\tau_{\text{em}}$  is the characteristic time of the density fluctuations in the transition state,  $\tau_t$ . So,  $\tau_{\text{em}} \approx (\tau_t^2 + \tau_n^2)^{1/2}$ . In earlier papers, the emission time was defined *only* by the time characteristic of density fluctuations in the system at the stage of fragment formation, i.e., at  $t \approx t_2$ . The actual picture is much more complex. What are the values of these characteristic times? Thermalization or energy relaxation time after intranuclear cascade,  $t_1$ , is model-estimated to be 10–20 fm/c. It is estimated previously that  $\langle t_2 - t_1 \rangle \approx 70$  fm/c for  $p(8.1 \text{ GeV}) + \text{Au}$  collisions. Calculation within the QMD model yields  $t_3$

equal to 150–200 fm/c. A new theoretical consideration of the partition dynamics of very hot nuclei is needed.

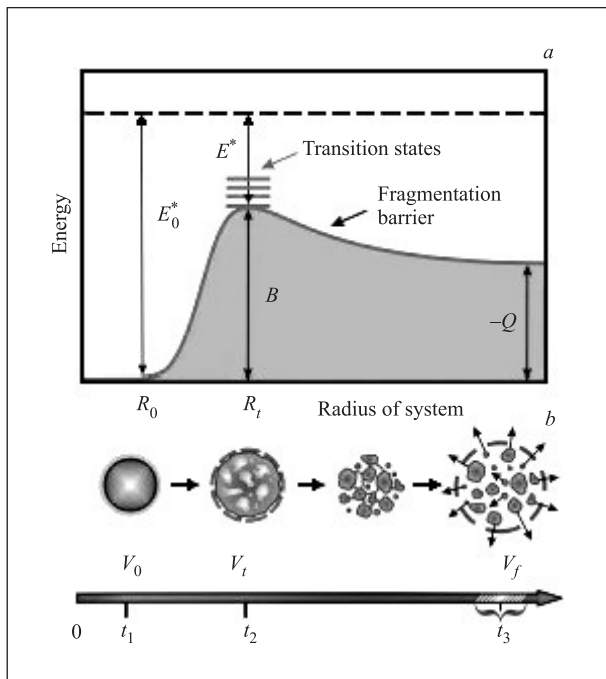


Fig. 14. a) Qualitative presentation of the potential energy of the hot nucleus (with excitation energy  $E_0^*$ ) as a function of the system radius. The ground-state energy of the system is  $E = 0$ ,  $B$  is the fragmentation barrier,  $Q$  is the released energy. b) Schematic view of the multifragmentation process and its time scale

## APPLIED SCIENTIFIC RESEARCH

The work on development of the **CYTRACK** cyclotron for track-membrane production was finished. Numeric simulations for the beam injection into the CYTRACK cyclotron were carried out and reported at the International Scientific Seminar in Memory of V.P. Sarantsev [32]. The work on the CYTRACK cyclotron development was awarded the JINR Second Prize for applied investigations.

In 2006 DLNP plans to restore the **JINR Phasotron** damaged by fire in 2005. After restoration the study of possibilities of forming a scanning proton beam for the radiotherapy, consideration of different variants of the beam channel for eye tumour treatment, and assessment of the possibility of accelerating  $^3\text{He}$  and  $^4\text{He}$  ions will be continued.

Under the JINR topic «**Physics and Technology of Particle Accelerators**», the LEPTA ring was tested with a pulsed electron beam [33]. Dependence of the lifetime of the circulating beam on different parameters of the ring was measured. It was found that the

But it is especially important to find a way to measure  $t_3$ . The fragment emission time  $\tau_{em}$ , as measured by the FASA collaboration in 2002, is  $\approx 50$  fm/c.

In the case of ordinary fission,  $t_2$  is specified by the fission width  $\Gamma_f$ , which corresponds to the mean time of the order of  $10^{-19}$  s (or  $\sim 3.3 \cdot 10^4$  fm/c) for the excitation energy around 100 MeV. The time  $t_3$  was model-estimated in a number of papers:  $t_3 \approx 1000$  fm/c. A mean neck rupture time is estimated within the model of Rayleigh instability:  $\tau_n = [1.5(R_n/\text{fm})^3]^{1/2} \times 10^{-22}$  s. Generally, the values of  $\tau_n$  are found to be less than 300 fm/c. Using this equation for the estimation of the mean time for the rupture of the multineck configuration in fragmentation, one gets  $\tau_n$  between 40 and 100 fm/c. This estimation is in a qualitative agreement with the measured values of the fragment emission time  $\tau_{em}$ . Thus, ordinary fission is characterized by much «slower» dynamics than multifragmentation. As for the space characteristics, the relative elongation of very heavy systems ( $Z > 99$ ) at the fission scission point is similar to that for the multiscission point of medium hot nuclei (rare-earth region). The essence of multifragmentation of hot nuclei is that fragments are formed as a result of the nuclear *liquid-fog* phase transition inside the spinodal region. But the dynamics of the whole process is very similar to that of ordinary fission.

In 2006 new experiments on the Nuclotron beam with the modified FASA setup will be performed to measure IMF-IMF relative velocity correlations. Analysis of the experimental data to get information about the pre-equilibrium emission in the multifragmentation process will be continued.

lifetime had specific dependence on energy (Fig. 15) — a smooth function  $\tau(\varepsilon)$  with a maximum around 4 keV.

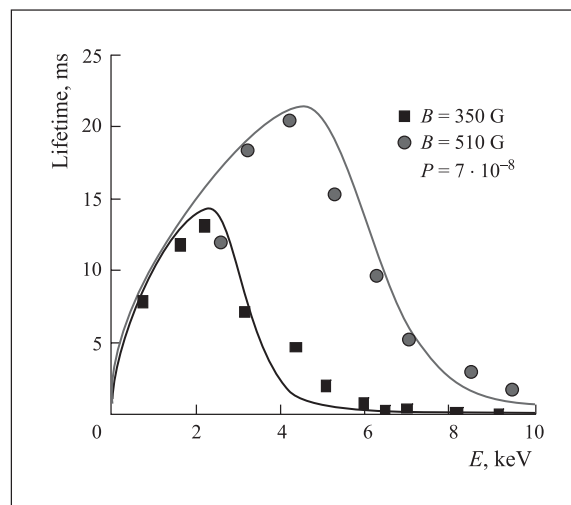


Fig. 15. Dependence of the circulating beam lifetime on energy

The left slope of the function curve  $\tau(\varepsilon)$  is related to lifetime limitation by electron scattering on residual gas atoms, the right slope — a decrease in the lifetime with energy — was explained by the influence of the inhomogeneities of the longitudinal focusing magnetic field. The maximum lifetime obtained in the experiments was equal to 22 ms (about  $5 \cdot 10^4$  turns). The positron injector was tested with positrons from the  $^{22}\text{Na}$  source of a low (0.8 MBq) activity. Moderation of the positron velocity in the microlayer of neon condensed at 10 K was studied. The test of the positron trap with electrons was started.

In 2006 it is planned to increase of the beam lifetime in the LEPTA ring by several orders of magnitude, to develop injection of positrons into the LEPTA ring, and to begin experiments on electron cooling of positrons.

The main goal of the topic «**Further Development of Methods and Instrumentation for Radiotherapy and Associated Diagnostics with the JINR Hadron Beams**» is to carry out medicobiological and clinical investigations on cancer treatment, to improve equipment and instrumentation, and to develop new techniques for treatment of malignant tumours and for associated diagnostics with medical hadron beams of the JINR Phasotron in a Medico-technical Complex (MTC) of DLNP [34]. In 2005, in collaboration with the Medical Radiological Research Centre (Obninsk), the Radiological Department of the Dubna hospital, and medical research centres of the Czech Republic and Bulgaria, the research on proton therapy of cancer patients with the Phasotron beams in treatment room No. 1 of MTC was continued. It was planned to carry out six treatment sessions during 2005, but unfortunately, because of the fire accident, that occurred in April in one of the Phasotron buildings, only one accelerator run was carried out. Twenty-two patients received fractionated course of treatment with the medical 150 MeV proton beam. Another 49 patients were irradiated with the Co-60 gamma unit Rokus-M (about 2000 single irradiations). The beam test of a removable deck to the therapeutic chair for patient setup in the supine position during proton radiotherapy was carried out. It will allow irradiation of a new class of tumours such as prostate cancer. A set of radiobiological experiments on investigation of «bystander» and «hypersensitivity» effects and of combined optical and ionizing radiation action on the mouse cells were carried out with the proton beam and gamma radiation. Investigations on the molecular analysis of radiation-induced mutations in animal and human genes were continued. The computer simulation of 3D genome macroarchitecture in irradiated animal germ cells with the «position effect» of gene was started.

In 2006 it is planned to complete the restoration of the equipment of the therapeutic proton beam lines which were damaged in the fire accident, to align the magnetic elements of the beam line and to deliver the therapeutic proton beam with the required characteristics to treatment room No. 1. The research on pro-

ton therapy of cancer patients with the JINR Phasotron beams in MTC's treatment room No. 1 will be continued. The developed technique of prostate cancer treatment with the proton beam will be tested. Development of a hardware and software complex based on an amorphous silicon flat panel detector for verification of patients setup during proton therapy will be started. The investigations on the molecular analysis of radiation-induced mutations in genes and on 3D simulation of genome macroarchitecture will be continued.

## REFERENCES

1. *Bellettini G. et al.* JINR Commun. E1-2005-131. Dubna, 2005.
2. *Adelman J. et al.* Top Quark Mass Measurement Using the Template Method in the Lepton + Jets Channel at CDF II. CDF/PHYS/TOP/CDFR/7532. 2005.
3. *Bellettini G. et al.* Top Mass Measurement in Dilepton Events Using Neutrino Phi Weighting Method. CDF/PHYS/TOP/GROUP/7641. 2005.
4. *Bellettini G. et al.* JINR Commun. E1-2005-129. Dubna, 2005.
5. *Ambrose D. et al.* Measurement of Top Quark Mass Using Template Methods on Dilepton Events. CDF/PUB/TOP/CDFR/7919. 2005.
6. *Giokaris N. et al.* Probing the Top Quark Mass in the Dilepton and Lepton + Jets Channels Using Only Lepton Information. CDF/PUB/TOP/PUBLIC/7888. 2005.
7. *Giokaris N. et al.* JINR Commun. E1-2005-104. Dubna, 2005.
8. *D0 Collab.* Measurement of the Isolated Photon Cross Section in  $p\bar{p}$  Collisions at  $\sqrt{s} = 1.96$  TeV. hep-ex/0511054.
9. *Adeva B. et al.* First measurement of the  $\pi^+\pi^-$  atom lifetime // Phys. Lett. B. 2005. V. 619. P. 50.
10. *Budagov J. et al.* Electromagnetic Energy Calibration of the TILECAL Modules with the Flat Filter Method (July 2002 Test Beam Data). ATL-TILECAL-PUB-2005-003; CERN-ATL-COM-TILECAL-2005-006. 2005.
11. *Kulchitsky Y. et al.* Energy Calibration of the TILECAL Modules with the Fit Filter Method (July 2002 Test Beam Data). ATL-TILECAL-PUB-2005-005; CERN-ATL-COM-TILECAL-2005-008. 2005.
12. *Kulchitsky Y. et al.* Electron Energy Resolution of the ATLAS TILECAL Modules with Flat Filter Method (July 2002 Test Beam Data). ATL-TILECAL-PUB-2005-004; CERN-ATL-COM-TILECAL-2005-007. 2005.
13. *Catanesi M. G. et al.* Measurement of the Production Cross-Section of Positive Pions in  $p\text{-Al}$  Collisions at 12.9 GeV/c. hep-ex/0510039.
14. *Arbuzov A. et al.* One-loop corrections to the Drell-Yan processes in SANC (I). The charged current case. hep-ph/0506110.
15. *Bardin D. et al.* SANCnews: Sector f f b b. hep-ph/0506120.
16. *Cordero A. et al.* // Proc. of the 29th ICRC, Pune, 2005 (in press).

17. *Abrashkin V. et al.* Advances in space research // Proc. of COSPAR-2005 (in press).
18. *Podorozhnyi D. et al.* // 29th Intern. Cosmic Ray Conf., Pune, 2005 (in press).
19. *Arnold R. et al.* // Phys. Rev. Lett. 2005. V. 95. P. 182302.
20. *Dudkin G.N., Bystritsky V.M., Bystritskii Vit.M.* Neutron emission at plasma flow collision across of external magnetic field // Plasma Phys. 2005. V. 31. P. 1.
21. *Bystritsky V.M. et al.* Study of the  $pd$  reaction at ultralow energies using hydrogen liner plasma // Phys. At. Nucl. 2005. V. 68. P. 1777.
22. *Korenchenko S.M. et al.* Deviation from the standard model in the decay  $\pi^+ \rightarrow e^+ \nu \gamma$  // Ibid. P. 498–507; Yad. Fiz. 2005. V. 68. P. 527–536.
23. *Filchenkov V.V. et al.* Influence of the Epithermal Effects on the MCF Steady State. JINR Preprint E15-2005-22. Dubna, 2005.
24. *Yaschenko S. et al.* // Phys. Rev. Lett. 2005. V. 94. P. 072304.
25. *Uzikov Yu.* // J. Phys. G. 2002. V. 28. P. B13.
26. *Komarov V. et al.* // Phys. Lett. B. 2003. V. 553. P. 179.
27. *Brudanin V.B. et al.* Search for double electron capture of  $^{106}\text{Cd}$  in the experiment TGV-2 // Izv. RAN. Ser. fiz. (in press).
28. *Batusov Yu.A. et al.* Resonant behaviour in double charge exchange reaction of  $\pi^+$ -mesons on the nuclear photoemulsion // Eur. J. Phys. (submitted).
29. *Angelov N. et al.* On the muon neutrino mass // Eur. J. Phys. (submitted).
30. *Karnaikhov V.A. et al.* // Nucl. Phys. A. 2005. V. 749. P. 65c.
31. *Budzanowski A. et al.* // Acta Phys. Polon. 2005. V. 36. P. 1203.
32. *Denisov Yu. et al.* Bancher of the cyclotron CYTRACK, simulations and experiment // Proc. of VI Intern. Sci. Seminar in Memory of V.P. Sarantsev, Dubna, 2005 (in press).
33. *Kobets A.G. et al.* Perspectives of LEPTA // Proc. of the VIII Intern. Conf. on Low Energy Antiproton Phys. (LEAP'05), Bonn, Germany, May 16–22, 2005. P. 399–405.
34. *Gulidov I. et al.* Proton therapy at Dubna // Radiotherapy & Oncology. 2005. V. 76. P. 159.